INTERNATIONAL JOURNAL OF CLIMATOLOGY
Int. J. Climatol. (2017)
Published online in Wiley Online Library
(wileyonlinelibrary.com) DOI: 10.1002/joc.5010

RMetS
Royal Meteorological Society

Exploring the feasibility of empirical, dynamical and combined probabilistic rainy season onset forecasts for São Paulo, Brazil

Caio A. S. Coelho,[a]* Mári A. F. Firpo,[a] Aline H. N. Maia[b] and Craig MacLachlan[c]

[a] *Centro de Previsão de Tempo e Estudos Climáticos (CPTEC), Instituto Nacional de Pesquisas Espaciais (INPE), Cachoeira Paulista, SP, Brazil*
[b] *Empresa Brasileira de Pesquisa Agropecuária (EMBRAPA) Meio Ambiente, Laboratório de Geotecnologias e Métodos Quantitativos, Jaguariúna, SP, Brazil*
[c] *Met Office Hadley Centre, Exeter, UK*

ABSTRACT: This study investigates the feasibility and presents an assessment of probabilistic rainy season onset forecasts for São Paulo, Brazil, located in a region with a well-defined wet season from mid-austral spring (October) to austral autumn (March/April). The probabilistic forecasts were produced with (1) a simple empirical Cox-regression model using July Niño-3 index as predictor, (2) the dynamical coupled atmosphere-land-surface-ocean-sea-ice model used in the UK Met Office Global Seasonal Forecast System (GloSea5) and (3) a procedure that combines the empirical and dynamical model onset probabilistic forecasts. The probabilistic forecast assessment was performed over the 1996–2009 retrospective forecast period for the event rainy season onset earlier (or later) than the historical (mean) onset date. The three investigated approaches resulted in similar discrimination ability of around 80%, which represents the probability of the probabilistic forecasts correctly distinguishing earlier from a later than mean onsets, suggesting good potential for rainy season onset forecasts for São Paulo. The robustness of this assessment for an extended period (longer than 1996–2009) and for a region (20°S, 25°S, 45°W, 55°W) that includes the city of São Paulo was checked, reinforcing the validity of the obtained results at both local and regional scales.

KEY WORDS rainy season onset; probabilistic forecasts; empirical; dynamical and combined forecasts

Received 18 March 2016; Revised 21 December 2016; Accepted 3 January 2017

1. Introduction

Prior knowledge about possible advance or delay in the rainy season onset is an important societal demand of several sectors including agriculture, water resources, energy production and public health. These sectors are constantly looking for advanced forecasts about rainy season characteristics to guide strategic decisions. Due to the complex nature and behaviour of weather and climate systems and associated uncertainties, probabilistic assessments are naturally more appropriate for addressing rainy season onset timing. Rather than forecasting the date when it is most likely the rainy season onset to occur, probabilistic forecast models are able to indicate the likelihood of an earlier or later than normal (climatological) rainy season onset date or an earlier or later onset than any pre-defined threshold dates.

Rainy season onset forecasting research has received great attention in recent years. Lo *et al.* (2007) developed a probabilistic logistic regression model to forecast the rainy season onset of the north Australian wet season. Lagged predictor indices such as the Southern Oscillation Index (SOI) and tropical Pacific sea surface temperatures (SST) were tested for producing cross-validated hindcasts. For most north Australia, the produced hindcasts showed skill exceeding that of climatological forecasts. Moron *et al.* (2009) investigated the characteristics and skill of monsoon onset forecasts over Indonesia. A simple cross-validated multivariate regression model based on canonical correlation analysis, constructed using July tropical Pacific and Indian Ocean SSTs used as predictors for local-scale onset dates over Indonesia, exhibited promising hindcast skill. Jones *et al.* (2012) analysed the skill of onset and demise dates, duration and amplitude probabilistic forecasts of the South American monsoon system (SAMS). The National Centers for Environmental Prediction Climate Forecast System, reforecasts version 2 (CFSRv2) for the period 1982–2009, were used in this investigation. An index based on precipitation anomalies empirical orthogonal function was used to characterize the investigated SAMS features. The CFSRv2 model showed useful skill when forecasting seasonal changes in SAMS. More recently, Vellinga *et al.* (2013) investigated forecast skill of probabilistic rainy season onset forecasts of the West African monsoon produced with the

* Correspondence to: C. A. S. Coelho, Centro de Previsão de Tempo e Estudos Climáticos (CPTEC), Instituto Nacional de Pesquisas Espaciais (INPE), Rodovia Presidente Dutra KM 40, SP-RJ, Cachoeira Paulista, SP CEP 12630-000, Brazil. E-mail: caio.coelho@cptec.inpe.br

UK Met Office GloSea4 system (Arribas *et al.*, 2011). Tercile categories forecast probabilities for onsets occurring before, near and after the normal onset defined using four different indicators were assessed. Glosea4 showed modest discrimination skill at 2–3 months' lead time measured by relative operating characteristic (ROC) scores.

This article aims to contribute to these recent research developments on rainy season onset forecasting by addressing the following questions: Is it feasible to produce skilful probabilistic rainy season onset forecasts for São Paulo, Brazil? How good are these forecasts for São Paulo? Can we indicate whether or not the rainy season is more likely to be advanced or delayed in a particular year when compared to the normal (climatological) onset date for São Paulo, by incorporating large-scale information [e.g. El Niño-Southern Oscillation (ENSO)] into empirical models? The motivation for investigating rainy season onset potential skill for a specific location is that São Paulo has a valuable long historical daily precipitation record covering the 1934–2013 period (80 years). Such a long record allows a detailed historical rainy season onset diagnostics, and also permits the construction of empirical (statistical) models for assessing skill of onset forecasts. Although this historical record is specific for its location, it has climatological features which are representative of nearby locations within the State of São Paulo in the Southeast Brazil region – the most important economic region of Brazil with various sectors dependent on climate information, particularly rainy season characteristics such as onset. In this sense, the results and conclusions obtained for São Paulo are likely to be extensible for nearly locations, providing a more regional representation. In fact, by using gridded precipitation daily data over a region that includes the city of São Paulo, it was possible to demonstrate the validity of the results and conclusions here documented both at local and regional scales (see Section 4). For all these reasons, the investigation of potential skill of rainy season onset predictions for São Paulo is a valuable and important endeavor.

In order to address the questions raised above a three-step approach is taken. First, an empirical probabilistic model (Maia and Meinke, 2010) is fitted to historical onset series for investigating the influence of ENSO on the probabilities of early or late rainy season onsets. Next, the forecasts of this empirical model are compared with the corresponding probabilistic forecasts produced by the UK Met Office seasonal forecast system, GloSea5 (MacLachlan *et al.*, 2015), which uses a dynamical model, for a common retrospective period (1996–2009). Finally, the onset forecasts produced by the empirical and the dynamical (GloSea5) models are combined and the resulting forecasts are assessed and compared with the skill of each individual model.

This article is organized as follows. Section 2 presents an exploratory and descriptive analysis of the annual rainfall and rainy season climatological features in São Paulo, Brazil, including the investigation for potential large-scale rainfall predictors. Section 3 describes the empirical model proposed by Maia and Meinke (2010) to produce probabilistic rainy season onset forecasts for São Paulo. Section 4 describes the UK Met Office seasonal forecast system, GloSea5, and derived probabilistic rainy season onset forecasts for São Paulo. Section 5 assesses skill and proposes a procedure for combining onset forecasts from empirical and dynamical models into a single consolidated forecast. Section 6 summarizes the main findings and presents the conclusions of the study.

2. Annual rainfall and rainy season climatology features in São Paulo

This study uses the observed precipitation recorded during the period 1934–2013 in the meteorological station of the Institute of Astronomy, Geophysics and Atmospheric Sciences (IAG) of the University of São Paulo (USP), located in São Paulo, Brazil. Figure 1(a) illustrates that the city of São Paulo has a well-defined dry period from April to September, with monthly mean precipitation lower than 100 mm, and a well-defined wet period from October to March, with monthly mean precipitation exceeding 150 mm, particularly during the peak months of rainy season (December, January, February and March). The rainy season onset is generally observed around the period from September to November, when precipitation starts to increase in São Paulo (Figure 1(a)). August is therefore a key month for rainy season onset forecasts. In order to be able to issue a rainy season onset forecast in August one needs to search for lagged climate predictors observed prior to August.

SSTs are recognized as key climate modulators and are therefore generally the first candidate predictors in climate prediction studies. Figure 1(c) shows a correlation map between September to November (SON) accumulated precipitation time series recorded in São Paulo (Figure 1(b)) and the previous July SST over the period 1934–2013. This analysis highlights the previous July SSTs in the Niño-3 region (illustrated by the rectangle in Figure 1(c)) as potential predictors for SON precipitation in São Paulo through positive association between SSTs in the eastern equatorial Pacific and precipitation. In other words, warming in July in the eastern equatorial Pacific (Niño-3 region), generally associated with El Niño conditions, is found to be consistent with increased precipitation in the following SON in São Paulo. Conversely, cooling in July in the Niño-3 region, generally associated with La Niña conditions, is found to be consistent with decreased precipitation in the following SON in São Paulo. This teleconnection response to the ENSO phenomenon is similar to the one usually observed in southern Brazil (Grimm *et al.*, 1998), a region that generally experiences increased precipitation during El Niño and reduced precipitation during La Niña conditions.

Figure 2 shows an example of observed daily precipitation during El Niño conditions [panels (a) and (c)] and during a weak cooling period in the Pacific resembling La

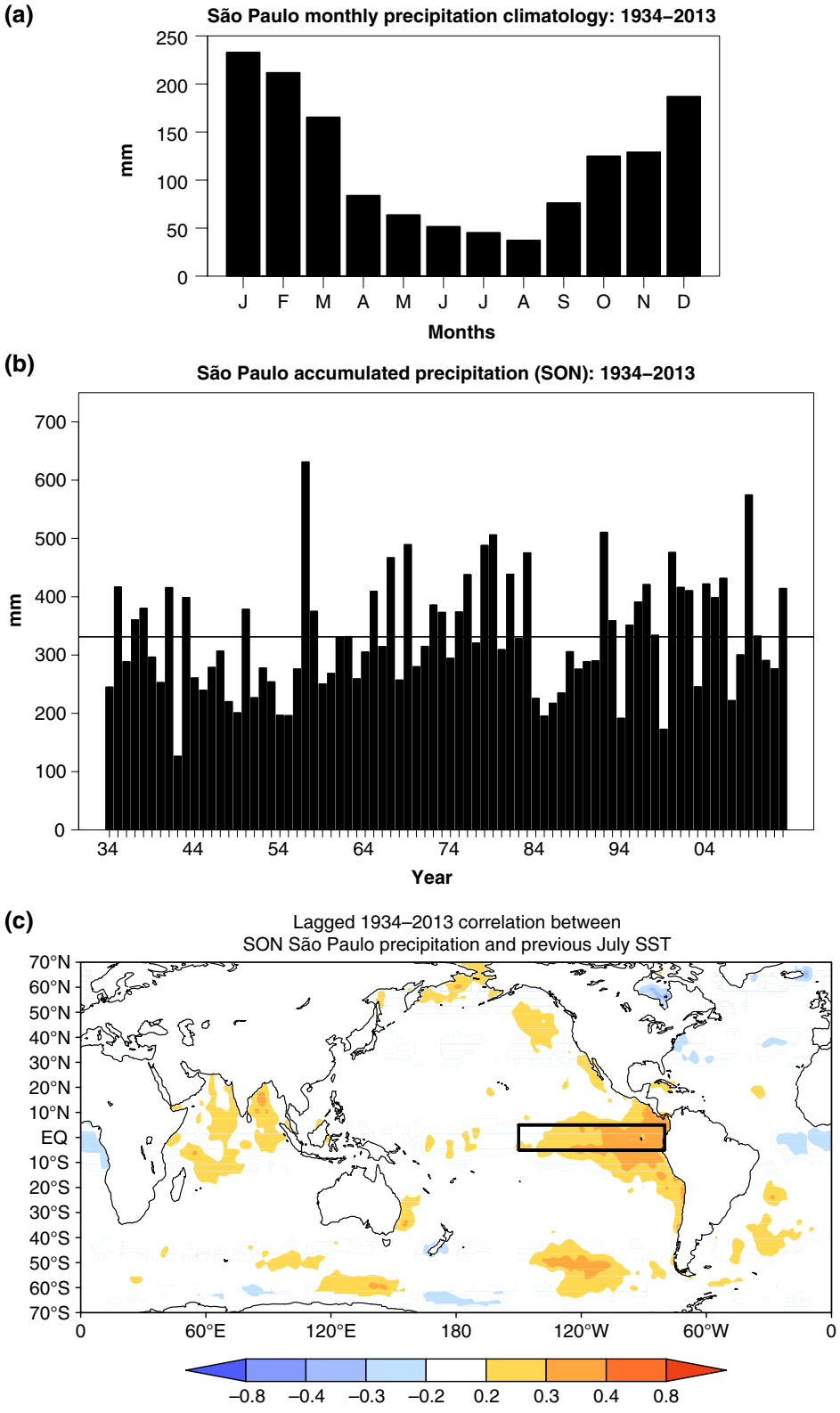

Figure 1. (a) São Paulo monthly mean precipitation for the period 1934–2013 computed using observations recorded at the meteorological station of the Institute of Astronomy, Geophysics and Atmospheric Sciences (IAG) of the University of São Paulo (USP), latitude 23°39′04″S, longitude 46°37′21″W, altitude 802 m. (b) São Paulo accumulated (September, October, November, SON) precipitation time series (1934–2013). (c) Correlation between SON precipitation in São Paulo and July sea surface temperatures (HadISST, Rayner *et al.*, 2003) over the period 1934–2013. Statistically significant correlation coefficients at the 5% level are shaded. The rectangle in the eastern equatorial Pacific illustrates the Niño-3 region (5°N–5°S, 150°–90°W).

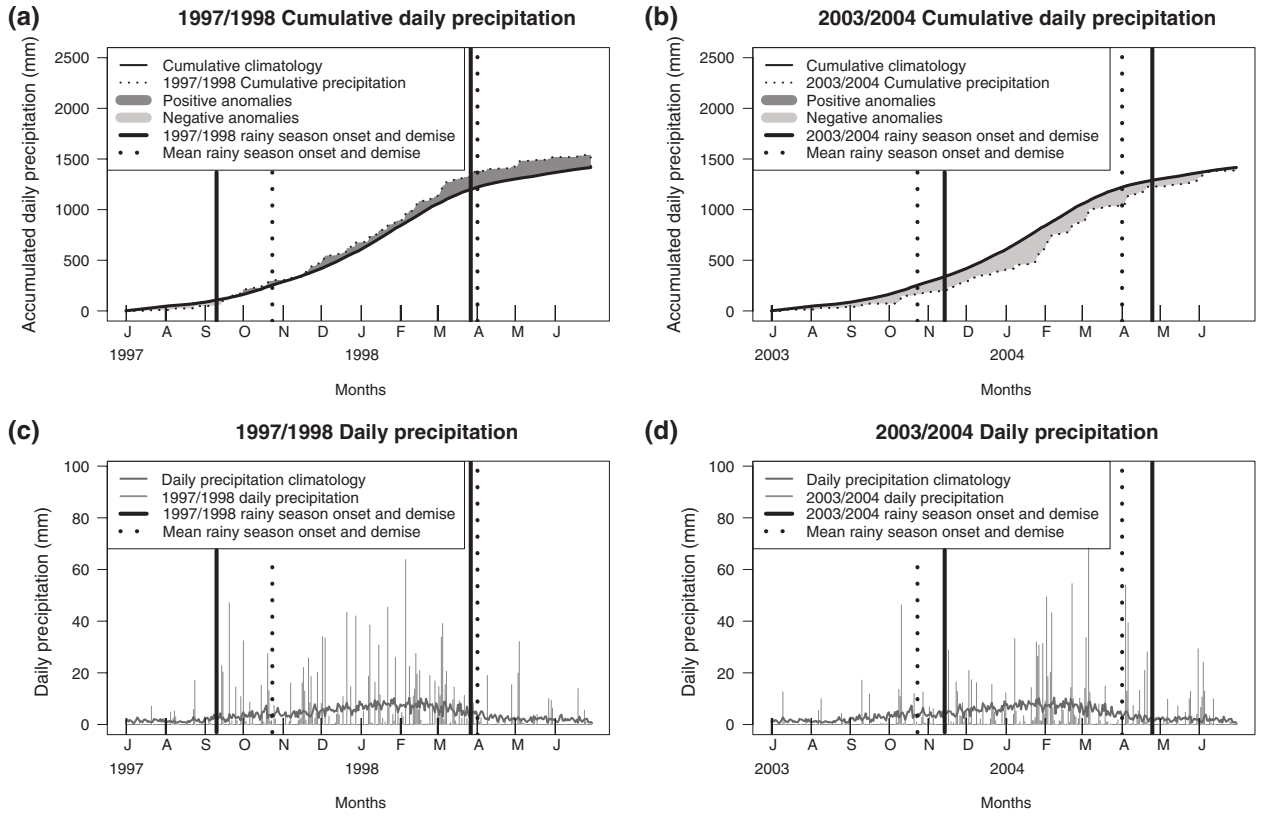

Figure 2. (a) São Paulo cumulative daily precipitation from 1 July to 30 June. The thick black solid line is the cumulative climatology for the period 1934/1935 to 2013/2014. The thin black solid line is the cumulative precipitation observed in 1997/1998 (i.e. from 1 July 1997 to 30 June 1998). (b) Same as (a) for 2003/2004. (c) São Paulo daily precipitation from 1 July to 30 June. The thick grey solid line is the daily climatology for the period 1934/1935 to 2013/2014. The thin grey vertical bars are the daily precipitation values observed in 1997/1998 (i.e. from 1 July 1997 to 30 June 1998). (d) Same as (c) for 2003/2004. The black dashed vertical thick lines shown in the panels mark the mean onset and demise dates based on the 1934/1935 to 2013/2014 climatology. The black vertical thick lines shown in the panels mark the estimated onset and demise dates for the 1997/1998 and 2013/2014 seasons.

Niña conditions [panels (b) and (d)]. This figure shows that not only the precipitation amount observed in São Paulo is affected by ENSO conditions (i.e. increased during El Niño and decreased during La Niña), but also the rainy season onset timing patterns are affected by an early onset during El Niño and a late onset during La Niña. The rainy season onset and demise dates were estimated using the method described by Liebmann *et al.* (2007), illustrated in Figure 3. This method was directly applied to the local precipitation record and is similar to the earlier proposed method by Camberlin and Diop (2003), which was applied to the resulting leading principal component of an analysis of a group of meteorological stations.

The Liebmann *et al.* (2007) method searches for minimum and maximum values of anomalous daily precipitation accumulation (Figure 3) and has been recently used by Coelho *et al.* (2016) to diagnose onset and demise dates of recent rainy seasons in the southeast region of São Paulo State. Applying this method for the observed daily historical precipitation in São Paulo for the period 1934/1935 to 2013/2014 one can construct climatological probability density functions (PDFs) of onset and demise dates as illustrated in Figures 4(a) and (b), respectively. Figure 4(a) shows that historically, São Paulo rainy season onset has started as early as late July and as late as late December, with the mean (typical) onset around the end of October. The robustness of this latter estimation was investigated by looking at other methods, (Lo *et al.*, 2007; Moron *et al.*, 2009) and a variation of the Liebmann *et al.* (2007) method restricted to the June to December period. The majority of the investigated approaches and the recent study by Coelho *et al.* (2016) agree in identifying the mean onset for São Paulo in late October, which has also been reported by others previous studies (e.g. Alves *et al.*, 2005; Franchi*to et a*l., 2008). The wide range of possible onset dates, characterized by a highly spread PDF (Figure 4(a)), highlights the challenge of precise onset predictions. Such uncertainty patterns call for the use of a probabilistic approach for assessing the risk (through probabilities) of onset to occur earlier or later than a pre-define date, rather than point forecasts of onset dates (i.e. exact onset forecast dates). Although the focus of this study is on rainy season onset, for completeness Figure 4(b) shows that historically, São Paulo rainy season demise has started as early as early January and as late as mid June, with the mean demise around the end of March/early April. Figure 4(c) refers to the dynamical model used in this study and will be discussed in Section 3.3.

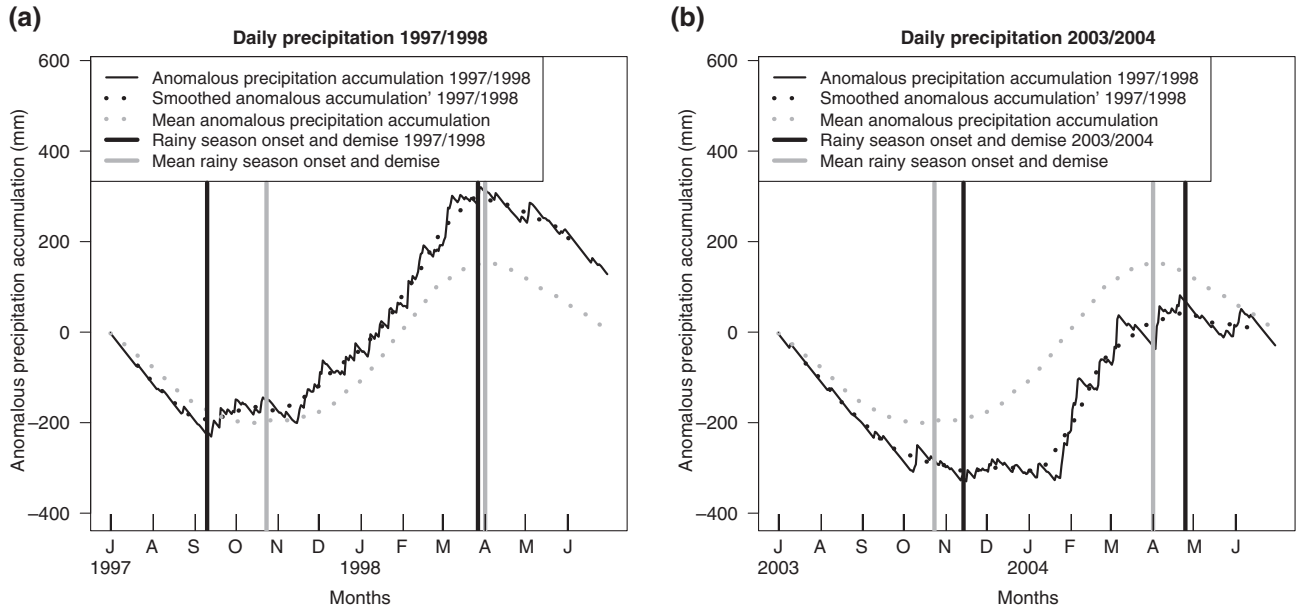

Figure 3. São Paulo anomalous daily precipitation accumulation in mm (solid black curve) for the period from (a) July 1997 to June 1998 and (b) July 2003 to June 2004. The black dotted line is the smoothed anomalous accumulation obtained applying a 41-days centred moving average. The first vertical solid black lines locate the estimated rainy season onset dates in 1997 and 2003. The second vertical solid black lines locate the estimated rainy season demise dates in 1998 and 2004. The dashed grey curve is the climatological mean anomalous daily precipitation accumulation for the period from 1934/1935 to 2013/2014. The first and second vertical solid grey lines locate the estimated rainy season onset and demise climatological dates.

3. Cox-regression model for probabilistic rainy season onset forecasts

3.1. Model formulation

The Cox-regression model (Cox, 1972), widely used in the medical literature when investigating risk factors associated to patient time to death, was introduced in climate science by Maia and Meinke (2010). This flexible non-linear, probabilistic, semi-parametric model is used here for investigating the feasibility of issuing rainy season onset forecast probabilities for São Paulo occurring earlier or later than a pre-defined onset date. The proposed Cox-regression model is written as:

$$P\left(T > t|\boldsymbol{x_i}\right) = P_o\left(T > t\right)^{\exp\left(\beta \cdot x_i'\right)} \qquad (1)$$

where $P(T > t|\boldsymbol{x_i})$ is the conditional probability of exceedance function (PEF), T is the response variable (time to rainy season onset, after 1 July), $P_o(T > t)$ is the baseline PEF, $\boldsymbol{x_i} = (x_{i1}, x_{i2}, \ldots x_{ij}, \ldots x_{ik})$ is a vector of climate indices used as predictors (covariates) and $\boldsymbol{\beta} = (\beta_1, \beta_2, \ldots \beta_i, \ldots \beta_k)$ is the vector of unknown model parameters corresponding to each predictor variable. $P_o(T > t)$ is estimated as one minus the empirical cumulative distribution function of the time to rainy season onset (T) arising from the historical onset time series. $P(T > t|\boldsymbol{x_i})$, as represented as $P(t|\boldsymbol{x_i})$ is interpreted as the probability for the rainy season onset to occur later than a particular value of t given the vector of predictor values $\boldsymbol{x_i}$ is known. The baseline P_o corresponds to the PEF in the absence of predictors (i.e. when $\beta = 0$). In climate science this baseline PEF is generally referred to as climatology. This model is semi-parametric due to the inclusion of a selected number of parameters β corresponding to each model predictor, without making assumptions about the underlying probability distribution function (e.g. normal, exponential and gamma) of the time to event (rainy season onset) variable T. The Cox-regression model of Equation (1) can be used to produce forecast probabilities or risks of the rainy season onset to occur later than any threshold onset time t given the vector of predictor values $\boldsymbol{x_i}$ with associated uncertainties of risk estimates. These forecast probabilities are expressed as the estimated $P(T > t|\boldsymbol{x_i})$ arising from the fitted Cox model.

The Cox model expressed in Equation (1) can also be represented in terms of a hazard function $[h(t|\boldsymbol{x_i})]$, which corresponds to the derivative of the corresponding PEF with respect to time to onset (t), written as:

$$h\left(t|\boldsymbol{x_i}\right) = h_o\left(t\right) \times \exp\left(\beta_1 \cdot x_{i1} + \beta_2 \cdot x_{i2} + \ldots \beta_k \cdot x_{ik}\right)$$

where $h_0(t)$ is the baseline hazard, $\beta_1, \beta_2, \ldots \beta_i, \ldots \beta_k$ are the unknown model parameters corresponding to each predictor variable and $x_{i1}, x_{i2}, \ldots x_{ij}, \ldots x_{ik}$ are the candidate predictors as defined in Equation (1). Briefly, the hazard function is the instantaneous event probability at a given time, or the probability that in a particular year, the time to onset occurs in a period centred around that point in time (Bradburn *et al.*, 2003a).

The variables $\boldsymbol{x_i} = (x_{i1}, x_{i2}, \ldots x_{ij}, \ldots x_{ik})'$ are generally large-scale climate indices chosen as candidate predictors for the $P(T > t|\boldsymbol{x_i})$. As illustrated in Figure 1(c), July Niño-3 SSTs are strongly correlated with the following SON accumulated precipitation in São Paulo, and therefore a potential predictor $\boldsymbol{x_i}$ for $P(T > t|\boldsymbol{x_i})$. A simple linear

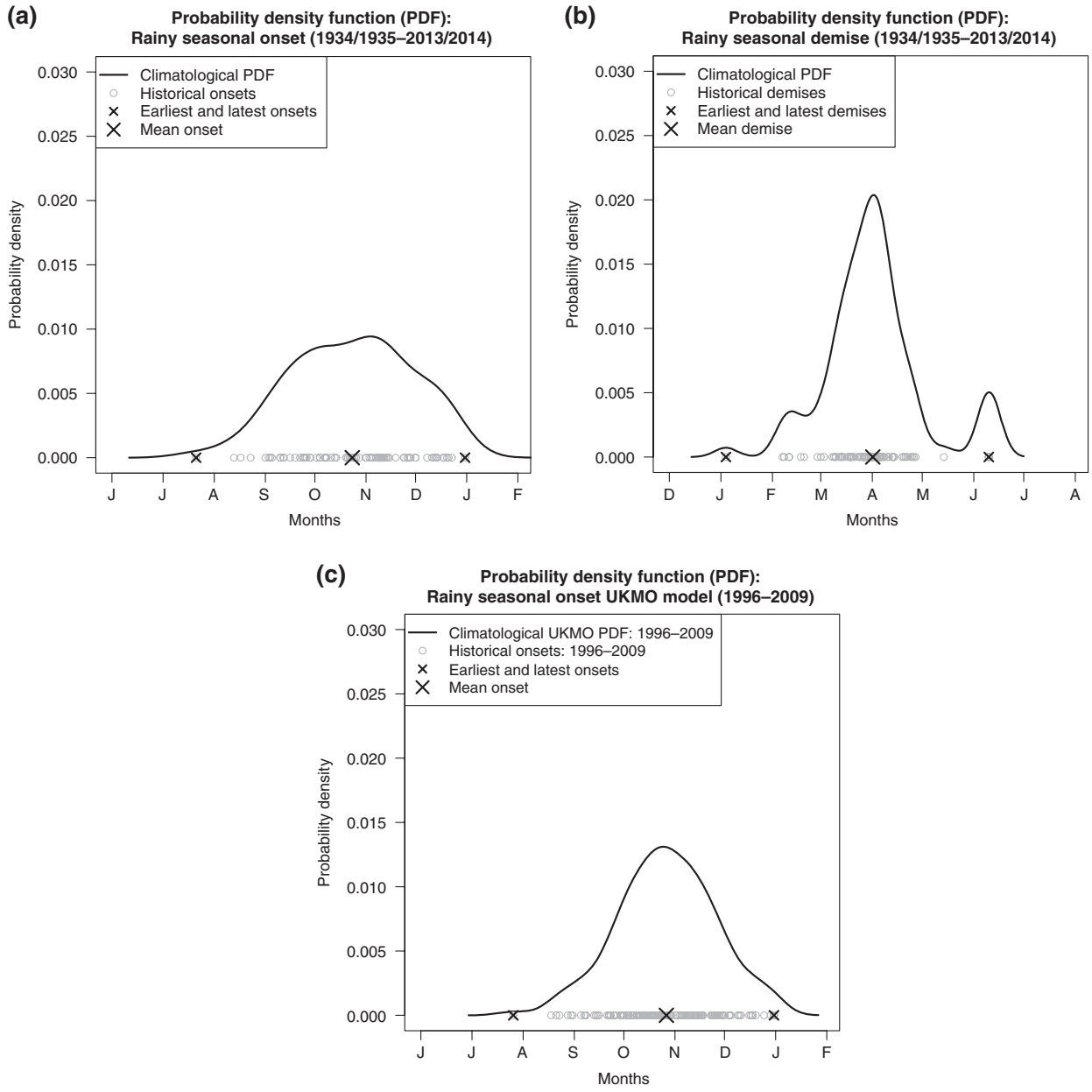

Figure 4. Probability density functions (PDFs) of rainy season (a) onset and (b) demise dates for São Paulo. Grey circles are historical dates for the period from 1934/1935 to 2013/2014. The solid line is the kernel pdf for the historical dates (grey circles). The large cross is the historical mean date for the period from 1934/1935 to 2013/2014. The small crosses are the earliest and latest onset and demise dates occurred in the period from 1934/1935 to 2013/2014. (c) PDF of rainy season onset retrospective forecast (hindcast) dates produced by the UK Met Office GloSea5 model (MacLachlan *et al.*, 2015) initialized in July during the period 1996–2009 for the area 22°–25°S, 45°–48,5°W, comprising six grid points of the model. Each grey circle represents one ensemble member.

analysis between July Niño-3 index and São Paulo rainy season onset dates (Figure 5) confirms such potential. A negative association between these two investigated variables (correlation coefficient of −0.35, p-value of 0.002) suggests that during El Niño years (here defined when Niño-3 SST in July are larger than 0.5 °C) the onset of the rainy season in São Paulo tends to be advanced. Conversely, during La Niña years (here defined when Niño-3 SST in July are smaller than −0.5 °C) the onset tends to be delayed. This feature is also illustrated by conditional PDF curves of the onset date (T) displayed to left and right of the scatter plot of Figure 5. After this investigation, July Niño-3 SST index has been chosen as a predictor ($\boldsymbol{x_i}$) for the probability of rainy season onset exceeding a threshold date (t) in São Paulo.

The positive estimate (0.34) of the Cox-model parameter β was found to be statistically significant and different from zero at the 6% significance level (p-value of 0.054) supporting the earlier finding that July Niño-3 index does have an impact on the time to onset variable t in São Paulo (Table 1). The interpretation of the β estimate in the Cox model is as follows. A unitary increase in the predictor July Niño-3 index ($\boldsymbol{x_i}$) results in the baseline P_o being powered to the positive estimate $\exp(\beta) = 1.41$. As P_o

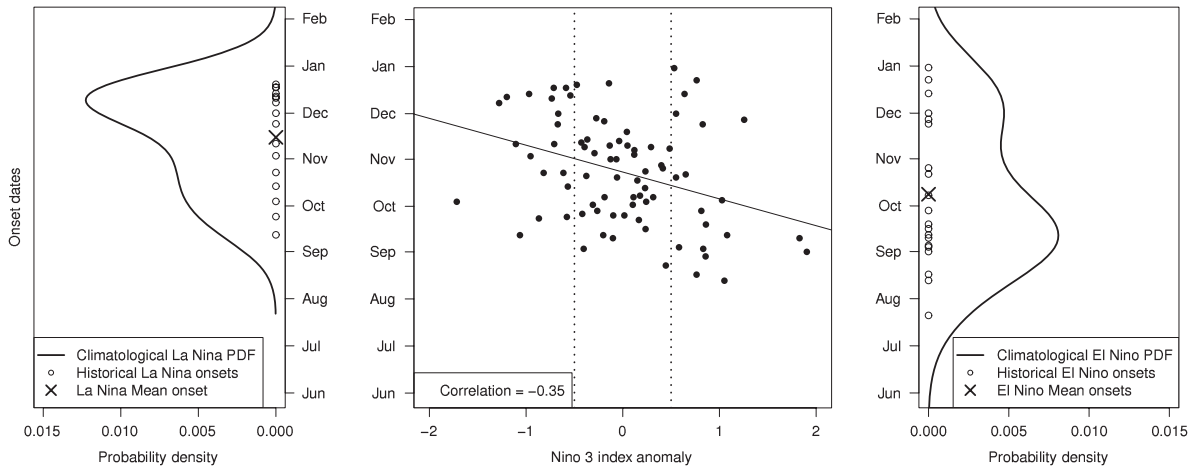

Figure 5. Scatter plot of July Niño-3 index against São Paulo rainy season onset dates estimated with the method proposed by Liebmann *et al.* (2007) for the period 1934–2013, with fitted linear regression (solid black line). The two curves to left and right of the scatter plot are conditional onset date pdfs on La Niña (Niño-3 index < -0.5) and El Niño (Niño-3 index > 0.5), respectively.

Table 1. Parameters of Cox-regression model $P(y|x_i)$ (Equation (1)) for time to rainy season onset y in São Paulo after 1 July using July Niño-3 index as predictor x_i estimated using data for the period 1934–2013.

β Estimate	β Estimate standard error	Estimate of hazard ratio: $\exp(\beta)$	p-Value
0.34	0.18	1.41	0.054

ranges from 0 to 1 this leads to a decrease in $P(t|\boldsymbol{x_i})$ when compared to $P_o(t)$. This means a decrease in the probability $P(T > t|\boldsymbol{x_i})$ for the onset to be later than any threshold onset time t given a positive unitary increase in the value of the predictor July Nino-3 index ($\boldsymbol{x_i}$) when compared to the baseline (climatological) probability $P_o(t)$. Generalizing this finding, when $\exp(\beta.\boldsymbol{x_i})$ is greater than one $P(T > t|\boldsymbol{x_i})$ will be less than $P_o(t)$. Conversely, a unitary decrease in the predictor July Niño-3 index ($\boldsymbol{x_i}$) results in the baseline P_o being powered to $\exp(-\beta) = 0.71$, leading to an increase in $P(t|\boldsymbol{x_i})$ when compared to $P_o(t)$. In other words when $\exp(\beta.\boldsymbol{x_i})$ is less than one $P(T > t|\boldsymbol{x_i})$ will be greater than $P_o(t)$.

3.2. Model assumption investigation

The Cox-regression formulation used here assumes proportional hazards in the sense that the hazard functions for the any value of $\boldsymbol{x_i}$ should be proportional and these functions should not cross each other. Proportionality implies that the quantities $\exp(\beta_i)$, called hazard ratios, do not change over time (Bradburn *et al.*, 2003b). In our example, it implies that the impact of the predictor Niño-3 index $\boldsymbol{x_i}$ on the risks associated with the time to rainy season onset (t) do not change over time and are proportional in strength, for example, during El Niño and La Niña conditions.

In order to examine this assumption, a diagnostic analysis was performed, comprising of: a plot of $\log(-\log(P(t|\boldsymbol{x_i})))$ *versus* the logarithm of time to onset ($\log(t)$) for three predictor values of the Niño-3 index $\boldsymbol{x_i}$ (Figure 6(a)) and a graph of scaled Schoenfeld residuals (Schoenfeld, 1982; Grambsch and Therneau, 1994) for the fitted Cox-regression model (Figure 6(b)). The first plot is known in the medical literature as the logarithm of minus the logarithm of the survival function, as the cumulative hazard is equal to the negative logarithm of the survival function, which in our study is given by $P(t|\boldsymbol{x_i})$. As described and reviewed by Maia and Meinke (2010) parallelism among the three curves as shown in Figure 6(a) indicates no evidence against the proportional hazards assumption.

The absence of linear trend over time in the scaled Schoenfeld residuals, here quantified by the p-value ($p = 0.94$) for the corresponding t-test for the slope of the black line in Figure 6(b), also indicates no evidence against the proportional hazards assumption. In our study, Schoenfeld residuals are interpreted as the difference between the observed and the expected values of the Niño-3 effect on the rainy season onset probabilities at each time (Hosmer and Lemeshow, 1999). The absence of trend then provides evidence that this effect is unchanged over time as originally postulated by the proportional hazards assumption. The Cox-regression model here proposed is therefore considered appropriate for investigating the feasibility of producing probabilistic rainy season onset forecasts for São Paulo, regarding both aspects: no violation of the proportional hazards assumption and the significance of the chosen predictor (July Niño-3 index) as discussed earlier.

3.3. Procedure for model skill assessment

For the skill assessment of the Cox-regression model using the July Niño-3 index as predictor shown hereafter the sample of historical records was first split in two parts: a training period (1934–1995) and a validation period (1996–2009). Next, the model parameters, including the estimated historical mean onset date that defines the binary

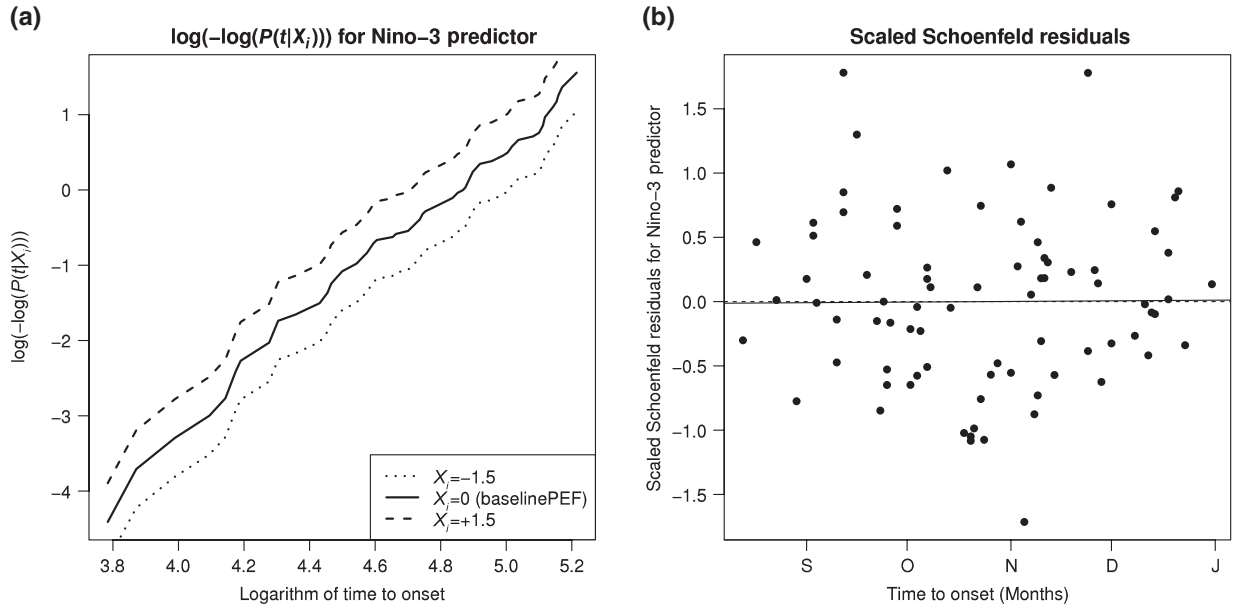

Figure 6. Diagnostics of non-proportionality. (a) Graphic of $\log(-\log(P(t|\boldsymbol{x}_i)))$ *versus* the logarithm of time to onset $\log(t)$ for three Niño-3 index predictor values ($x_i = -1.5$, $x_i = 0$ and $x_i = 1.5$). (b) Scatter plot of scaled Schoenfeld residuals *versus* time to onset, showing estimated linear trend (solid black line).

event of our interest, were estimated using data from the training period (1934–1995). After estimating the model parameters and the historical mean onset date using the training period data, these parameters were then used to make probabilistic forecasts for the remaining years of the validation period 1996–2009. The reason for splitting the historical record in these two periods is to allow the comparison of Cox-regression model forecasts with the corresponding forecasts for the dynamical model used in this study (see Section 4), which was only available over the 1996–2009 period.

For illustrating the use of the proposed Cox model with the July Niño-3 index as predictor ($\boldsymbol{x_i}$), Figures 7(a) and (b) show the forecast PEFs for the time to the rainy season onset in São Paulo, in two contrasting situations: forecasting the rainy season onset for 1997/1998 and 2003/2004 for which the previous July Niño-3 index values were 1.83 °C (El Niño conditions) and −0.37 °C (weak cooling resembling La Niña conditions), respectively. It is worth emphasizing that the Cox-regression model produces the full time-to-onset (T) forecast distribution conditioned on the predictor values ($\boldsymbol{x_i}$ = July Niño-3 index) as illustrated by the grey curves in Figures 7(a) and (b). The production of full forecast distribution contrasts with widely used approaches such as (multiple) linear regression, which is generally used to produce point estimates of T given $\boldsymbol{x_i}$ with an associated normal (Gaussian) predicted PDF, or logistic regression for producing forecasts of the $P(T > k|\boldsymbol{x_i})$ for a single value of k at a time. The latter approach was adopted in Lo *et al.* (2007) by producing multiple logistic fits to compose conditional predicted PEFs.

The 1997/1998 PEF forecast (grey curve) falls below the climatological PEF (black curve) indicating reduced probabilities for the rainy season onset to be later than any pre-defined threshold onset time t given the predictor July 1997 Niño-3 index when compared to the climatological probabilities (Figure 7(a)). By reading the probability of exceedance in the y-axis of Figure 7(a), one finds a Cox-regression forecast probability of 36% for rainy season onset to be later than the historical mean onset time (vertical black line), leaving 64% probability for the rainy season onset time to be earlier than the historical mean onset time. The 1997/1998 rainy season onset (large black dot in Figure 7(c)) was indeed observed earlier than the historical mean onset (large cross), illustrating that the Cox-regression forecast correctly indicated higher probability (64%) for an earlier than normal onset.

Figure 7(b) shows that in opposition to the earlier presented situation, the 2003/2004 PEF forecast (grey curve) falls above the climatological PEF (black curve), indicating increased probabilities for the rainy season onset to be later than any pre-defined threshold onset time t given the predictor July 2003 Niño-3. The Cox-regression forecast probability for the 2003/2004 rainy season onset to be later than the historical mean onset time (vertical black line) is 55%. The 2003/2004 rainy season onset (large black dot in Figure 7(d)) was indeed observed later than the historical mean onset (large cross in Figure 7(d)), illustrating that the Cox-regression forecast correctly indicated higher probability (55%) for a later than normal onset.

4. The UK Met Office GloSea5 probabilistic rainy season onset forecasts

The second step of the investigation consisted in examining rainy season onset probabilistic forecasts produced by the UK Met Office GloSea5 (MacLachlan *et al.*,

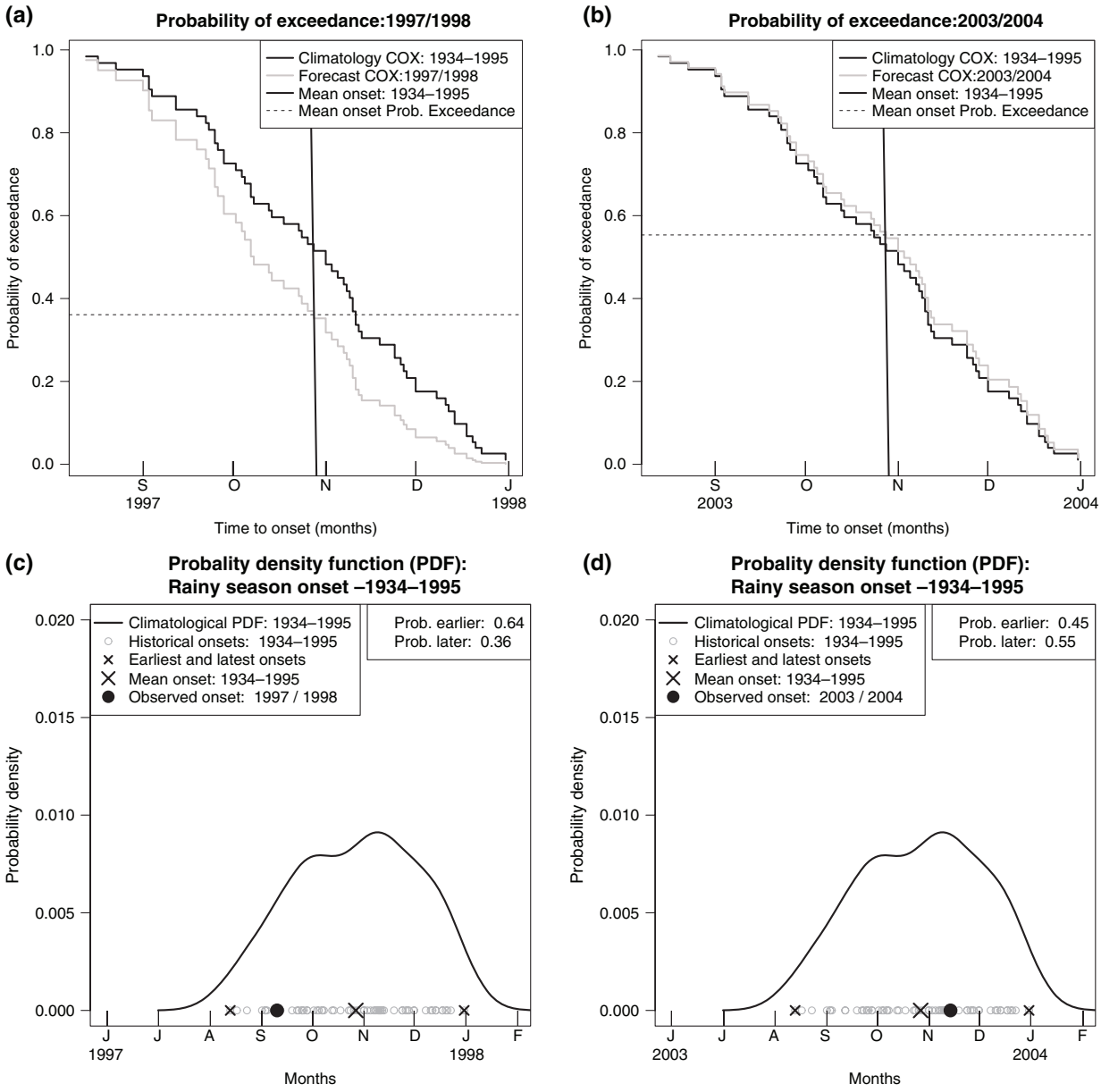

Figure 7. (a) Climatological probability of exceedance function (PEF) for the period 1934–1995 (black curve) and forecast PEF for the 1997/1998 rainy season onset for São Paulo based on the Cox-regression model described in Section 3 fitted over the 1934–1995 period using the July 1997 Niño-3 index of 1.83 °C as predictor (grey curve). (b) Climatological PEF for the period 1934–1995 (black curve) and forecast PEF for the 2003/2004 rainy season onset for São Paulo based on the Cox-regression model described in Section 3 fitted over the 1934–1995 period using the July 2003 Niño-3 index of −0.37 °C as predictor (grey curve). Probability density function (PDF, black curve) of rainy season onset dates (open grey circles) observed in São Paulo during the period 1934–1995 and the corresponding observed onset dates (black dot) during the (c) 1997/1998 and (d) 2003/2004 rainy seasons. The historical 1934–1995 mean onset is indicated with the large cross. The earliest and latest historical onsets are indicated with small crosses.

2015) system using all available data over the 14-year (1996–2009) retrospective period. GloSea5 is a recently developed state-of-the-art monthly to seasonal ensemble prediction system. It uses a high-resolution dynamical coupled atmosphere-land-surface-ocean-sea-ice model ($0.83° \times 0.56°$ in the atmosphere and 0.25° in the ocean). For each month of each of the 14 retrospective forecast years, a total of 12 ensemble member were produced by generating three different members for three different starting dates (the 1, 9, 17 and 25 day of the calendar) for the following 7 months. In this study, the 12 precipitation daily output ensemble members of the July starting dates for the area average between 22°S and 25°S and 45°W and 48.5°W, comprising six grid points of the model, which include the coordinates for the city of São Paulo were investigated. This regional averaging procedure was used to better extract the predicted signal from the model. For determining the rainy season onset for this 14 retrospective forecast years, the method described by Liebmann *et al.* (2007) was applied to daily precipitation forecasts of each of the 12 ensemble members of each year. The comparison between the rainy season onset

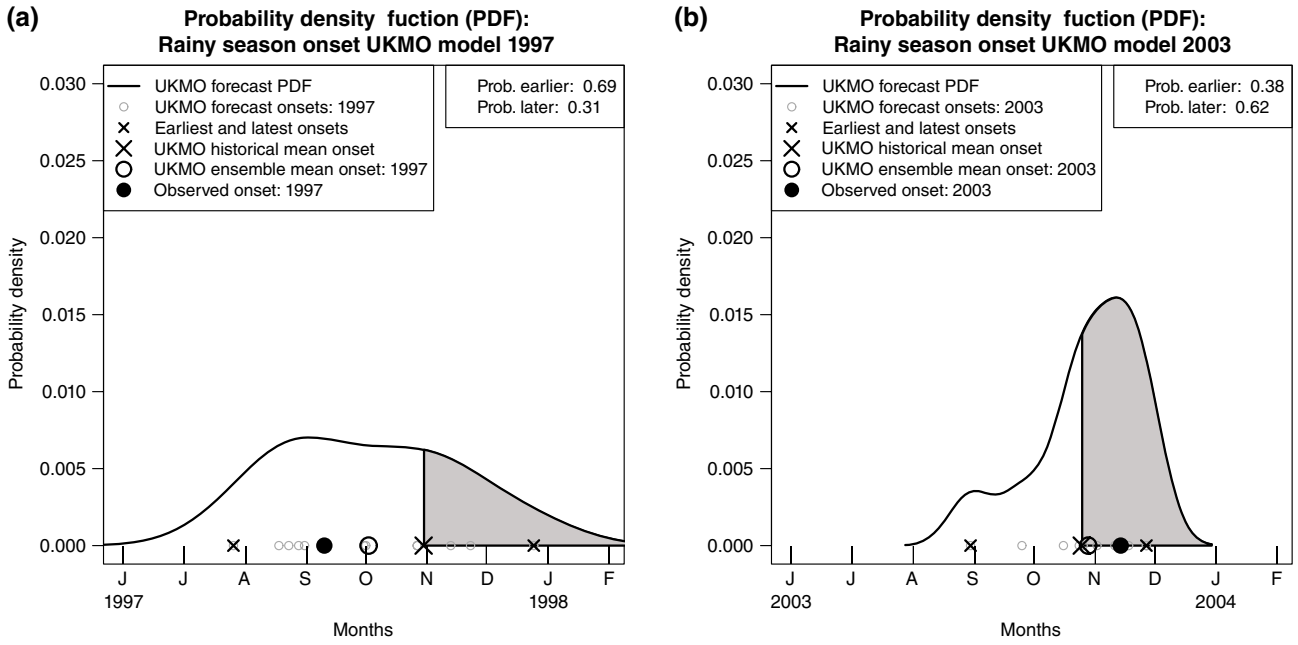

Figure 8. Kernel probability density function (PDF) forecast (black curve) derived from the UK Met Office GloSea 5 model for the (a) 1997/1998 and (b) 2003/2004 rainy season onset in São Paulo (area average over 22°–25°S, 45°–48.5°W, comprising six grid points of the model). Each grey circle represents an ensemble member. The black open circle is the forecast ensemble mean onset date. The small crosses represent the earliest and latest onset forecast dates. The large cross represents the historical mean onset for the UK Met Office GloSea 5 model computed in cross-validation leaving out 3 years (1996, 1997 and 1998 in panel (a) and 2002, 2003 and 2004 in panel (b) of the period 1996–2009 period). The back dots represent the observed onset dates.

PDFs produced by the GloSea5 model (Figure 4(c)) and the one arising from observed data (Figure 4(a)) reveals that dynamical model reproduced remarkably well the climatological rainy season onset features such as the mean (large cross) as well as the earliest and latest onset dates (small crosses).

Similarly to the examples explored in the evaluation of the empirical model in the previous section, Figures 8(a) and (b) show time-to-onset forecast PDFs derived from the UK Met Office GloSea5 model for the 1997/1998 and 2003/2004 rainy seasons in São Paulo, respectively. These forecast PDFs were produced with the 12 available ensemble members. This is recognized as a limited sample to estimate a PDF. However, this is the typical number of retrospective forecast ensemble members produced by global climate centres due to constrains in the available computational resources to increase this number. When producing real-time forecasts this sample size is typically four to five times larger, what substantially improves the PDF estimation. The grey area under the forecast PDFs (back curves) is the forecast probability for a later than the historical mean onset for the UK Met Office GloSea5 model, which is represented by the large crosses. The forecast shown in Figure 8(a) indicates 31% probability for the 1997/1998 rainy season onset time to be later than the historical mean, leaving 69% probability for the rainy season onset time to be earlier than the historical mean onset time. The large black dot in Figure 8(a) shows that the 1997/1998 rainy season onset was indeed observed earlier than the historical mean onset, illustrating that the GloSea5 forecast was able to correctly indicate higher probability (69%) for an earlier than normal onset. For the 2003/2004 rainy season (Figure 8(b)) the forecast probability for the onset to occur later than the historical mean is 62%, leaving 38% probability for the onset to occur earlier than the historical mean onset. The 2003/2004 rainy season onset was indeed observed later than the historical mean onset (as shown by the large black dot in Figure 8(b)), illustrating that the GloSea5 forecast was able to correctly indicate higher probability (62%) for a later than normal onset.

5. Skill assessment and combination procedure of probabilistic onset forecasts

The previous sections presented examples of rainy season onset forecasts produced with a simple empirical Cox-regression model and the high-resolution dynamical coupled ocean–atmosphere UK Met Office GloSea5 model. As the precipitation forecasts produced with GloSea5 are available for the 1996–2009 retrospective period, to allow comparison, this section assesses the skill of both empirical Cox-regression and GloSea5 rainy season onset forecast over this 14-year period. In order to perform this comparative assessment, the Cox-regression model was fit using São Paulo time-to-onset and Niño-3 index data for the 1934–1995 training period. Next, this fitted Cox-regression model was used to produce probabilistic rainy season onset forecasts for São Paulo for the 1996–2009 validation period (common to the available GloSea5 period) using as predictor Niño-3 index data for the same period.

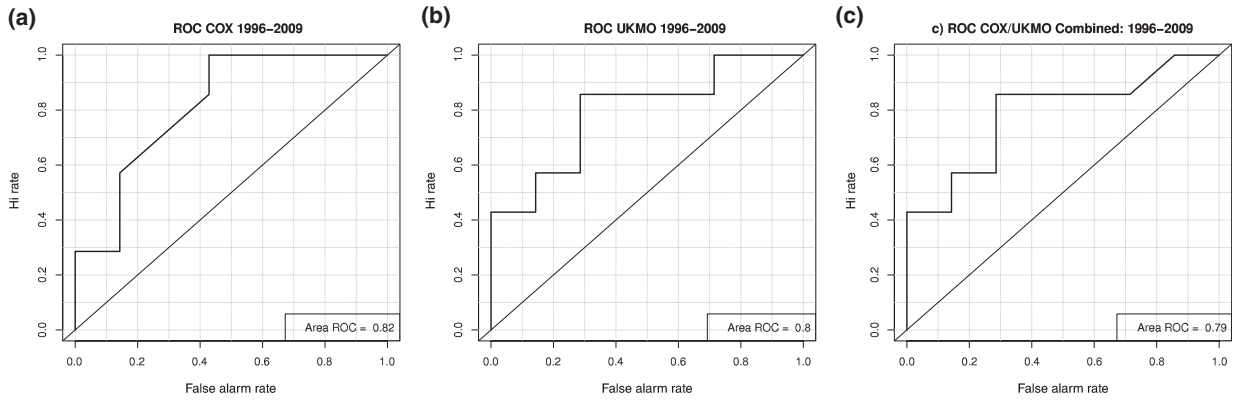

Figure 9. Relative operating characteristic (ROC) curve for (a) the empirical Cox-regression model using July Niño-3 as predictor, (b) the dynamical UK Met Office GloSea 5 model (area average over 22°–25°S, 45°–48.5°W, comprising six grid points of the model) and (c) the empirical-dynamical combination for the period 1996–2009.

The mean onset date used for producing probabilistic Cox-regression forecasts was computed for the 1934–1995 training period. For the dynamical model (GloSea 5), given the restricted (shorter) data availability, the mean onset date for each year was estimated using data for the 1996–2009 validation period in cross-validation mode, leaving 3 years out (of the 14 available years) at a time, being one of these 3 years the target forecast year. By computing the forecast probabilities for an earlier or later than mean onset for the 14 years as described above the biases of the dynamical model were largely intrinsically accounted. Although the mean onset dates used for producing empirical and dynamical probabilistic onset forecasts were different, both forecasts were produced for the common validation period (1996–2009) and were assessed against the same observations. This procedure minimized the impacts of the different mean onset estimates and allowed the comparison of forecasts produced by the two modelling approaches.

Similarly to the examples shown in Figures 7 and 8, forecast probabilities for the occurrence of a later than the historical mean onset were produced for both empirical Cox-regression and the dynamical GloSea5 models for all 14-years of the 1996–2009 period. The produced probability forecasts were used to assess the ability of each forecasting strategy in correctly discriminating earlier and later than historical mean rainy season onsets with the ROC curve (Mason, 1982). The ROC curve is obtained by plotting hit rates against false alarm rates computed for decreasing probability thresholds. The hit and false alarm rates are obtained from a two by two contingency table of forecast probabilities against binary observations of the event of interest. In this study, the event of interest is earlier (or later) than historical mean onset. Perfect forecasts have the area underneath the ROC curve equals to 100%, indicating perfect discrimination ability to distinguish earlier from later than historical mean onsets. Random (unskillful) forecasts have the area underneath the ROC curve equals to 50%, indicating completely absent discrimination ability. The areas underneath the ROC curves shown in Figures 9(a) and (b) indicate 82% and 80% probability of correctly discriminating earlier from later than historical mean onsets for the empirical and the dynamical model forecasts, respectively. This result indicates that the empirical and the dynamical models have similar discrimination ability.

One may question the reason why the obtained ROC skill for the non-linear Cox-regression model is apparently more impressive than the strength of the linear relationship between the predictor and predictand variables of this model. One of the reasons is that ROC is generally a more optimistic skill measure than correlation. These two measures assess different forecast quality attributes. ROC assesses discrimination for the non-linear Cox-regression model, a measure of how well the issued forecast probabilities distinguish events from non events, while correlation assesses linear association, with the strength of the latter being generally weaker than of the former. One of the advantages of using the probabilistic Cox model when compared to simple models that assume linear relationships between the predictor and the predictand is that the Cox model generally better captures the predictor *versus* predictand non-linear relationship. Another reason is that the strength of the relationship between the predictor and predictand is stronger in the validation period (1996–2009) when compared to the training period (1934–1995) of the empirical model (not shown).

Combining the individual probabilistic forecasts produced by the empirical Cox-regression and the dynamical GloSea5 models has the potential to improve discrimination ability. In order to explore this potential Figure 10 illustrates the proposed procedure for combining the probabilistic forecasts of these two models for the 2003 rainy season onset in São Paulo to be later than the mean onset into a single consolidated forecast. Both empirical and Cox-regression forecasts are expressed as a PEFs. In the example shown in Figure 10 the dark grey curve represents the empirical (Cox-regression) forecast expressed as PEF for the year 2003 using July 2003 Niño-3 index as predictor. The light grey curve represents the corresponding dynamical UK Met Office GloSea 5 forecast (average of six grid points over the area 22°–25°S, 45°–48.5°W)

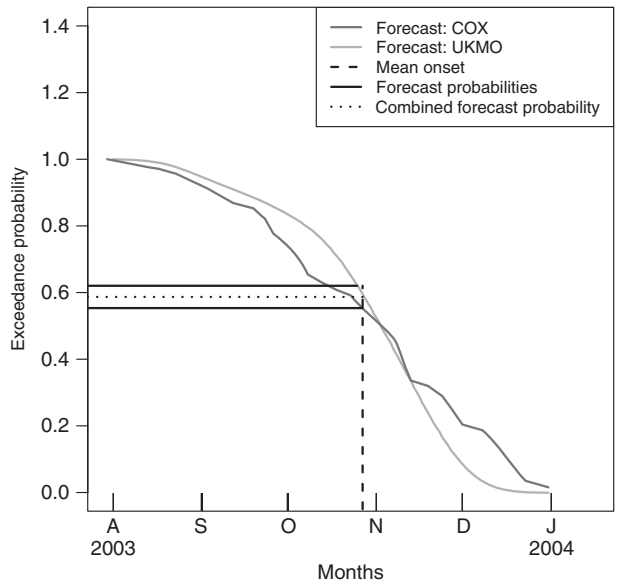

Figure 10. Illustration of the proposed procedure for combining empirical Cox-regression PEF using July Niño-3 as predictor (dark grey) and dynamical UK Met Office GloSea 5 PEF (area average over 22°–25°S, 45°–48.5°W, comprising six grid points of the model, light grey) probabilistic forecasts for the 2003 rainy season onset in São Paulo to be latter than the mean onset (vertical dashed line). The combined probabilistic forecast (horizontal short dashed line) is obtained by averaging the individual UK Met Office GloSea 5 and Cox-regression probabilistic forecasts represented by the first and second horizontal solid black lines, respectively.

expressed as PEF for the same year (2003) estimated using the 12 available ensemble members. Although the dynamical model forecast distribution (represented by the light grey curve in Figure 10) was estimated using a limited number of ensemble members, it can naturally be combined with the empirical model forecast distribution (represented by the dark grey curve in Figure 10), which is intrinsically obtained in the Cox regression. In such a procedure, what is being fairly compared and combined are the PEFs (dark and light grey curves), not a single (individual member) forecast coming from the observations with a 12 member ensemble forecast from the dynamical model. Figure 10 shows that the combined probabilistic forecast is obtained by averaging the individual GloSea5 and Cox-regression probabilistic forecasts for the onset to be later than the mean (historical) onset.

Figure 9(c) shows the ROC curve for the combined (empirical-dynamical) forecasts, which have an underneath area of 79%, indicating comparable ability to empirical (Figure 9(a)) and dynamical (Figure 9(b)) model forecasts in discriminating earlier from later than historical mean onsets. These results suggest that overall the three approaches (empirical, dynamical and combined) show similar discrimination ability of around 80% for successfully distinguishing earlier from later than historical mean onsets in São Paulo.

The robustness of the obtained results for a single location (the city of São Paulo) and its validity for an extended region was investigated by using Climate Prediction Center (CPC) daily $0.5° \times 0.5°$ data (Chen *et al.*, 2008) from 1979 to 2009 period averaged over the region 20°S, 25°S, 45°W, 55°W, which includes the city of São Paulo. The SON area average CPC precipitation over this region was found to have a similar positive correlation pattern with the previous July SST over the equatorial Pacific as illustrated in Figure 1(c). This suggests that the Niño 3 region is a good candidate predictor for SON precipitation not only in the city of São Paulo, but also over the region here investigated. The Cox-regression model with the previous July Niño 3 SST as predictor was then used to predict the probability of the onset to be later than the mean onset in the region 20°S, 25°S, 45°W, 55°W, over the 1979–2009 period, based on the CPC daily $0.5° \times 0.5°$ data. For this investigation, the cross-validation leave 1 year out procedure was performed. Figure 11(a) shows the ROC curve for these predictions, which have discrimination ability of 67% in distinguishing later from earlier than mean onsets. This result indicates that although smaller than the 80% discrimination ability identified for the local station in São Paulo, the identified ability is also valid for the region here investigated.

In order to further explore if for the city of São Paulo the 1996–2009 period was particularly favorable for the identified discrimination ability, we cross-validated (leaving 1 year out at a time) the Cox-regression model using previous July Niño-3 index as predictor over the 1934–2009 period. Figure 11(b) shows the ROC curve of this assessment, which indicates 63% discrimination ability in distinguishing later from earlier than the mean onsets. This result indicates that not only the 1996–2009 period shows skill in predicting this event. Although smaller than the 80% discrimination ability obtained for the 1996–2009 period, the identified positive ability (ROC area larger than 50%) is also valid for the longer cross-validated period (1934–2009), indicating that the result is sound and robust.

6. Summary and conclusions

This study explored the feasibility of producing probabilistic rainy season onset forecasts for São Paulo with three different approaches: (1) a simple empirical Cox-regression model, (2) the dynamical UK Met Office GloSea5 model and (3) by combining the forecasts of these two individual models into a consolidated forecast.

When searching for potential predictors for the use in the empirical model this study found an interesting and complementary finding to previous studies (e.g. Ropelewski and Halpert, 1987, 1989, 1996; Grimm *et al.*, 1998). These previous studies identified the impacts of ENSO on the observed precipitation in southern Brazil during austral spring, with increased precipitation during El Niño conditions and decreased precipitation during La Niña conditions. In this study, by using an 80-year long historical precipitation record for São Paulo, comprising the period from 1934 to 2013, it was possible to identify that the same ENSO impacts observed in southern Brazil are also experienced in São Paulo. The lagged correlation analysis

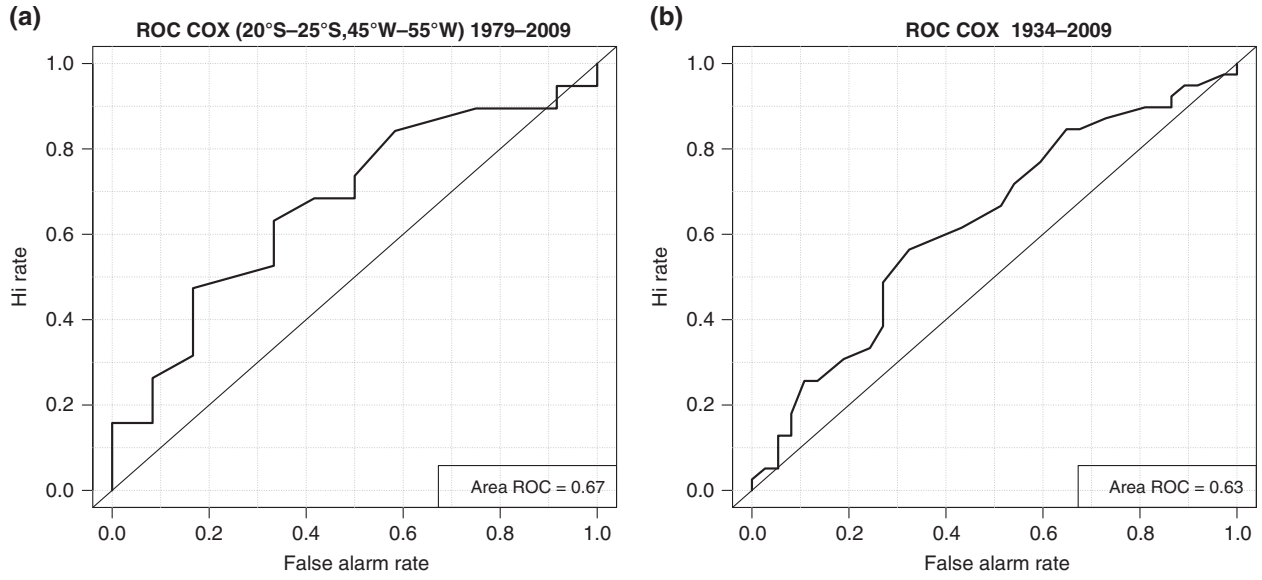

Figure 11. Relative operating characteristic (ROC) curve for (a) the empirical Cox-regression model fitted in cross-validation (leaving 1 year out at the time) over the 1979–2009 period for the Climate Prediction Center (CPC) average precipitation (Chen *et al.*, 2008) over the region 20°S, 25°S, 45°W and 55°W using July Niño-3 as predictor and (b) for the empirical Cox-regression model fitted in cross-validation (leaving 1 year out at the time) over the 1934–2009 period for the city of São Paulo using July Niño-3 as predictor.

revealed that El Nino conditions in July tend to increase precipitation in São Paulo in the following SON.

Conversely, this analysis also revealed that La Nina conditions in July tend to decrease precipitation in São Paulo in the following SON. Coelho *et al.* (2002) reported the State of São Paulo in the southeast region of Brazil as part of a transition region between the opposite ENSO impacts usually observed in southern and north/northeastern Brazil. The results of this new study suggest that the ENSO impact might not only be concentrated in southern Brazil, but might also be extended to southern parts of São Paulo State including the capital city of São Paulo here investigated.

The investigation of rainy season onset timing in São Paulo, identified by the method proposed by Liebmann *et al.* (2007), revealed that El Niño not only increased precipitation amount in São Paulo but also consistently advanced rainy season onset timing. Similarly, La Niña not only decreased precipitation amount in São Paulo, but also delayed rainy season onset timing. These novel results guided the application of the empirical Cox-regression model for probabilistic rainy season onset timing forecasts for São Paulo using the Niño-3 index in the previous July season as predictor. Such empirical model has the advantage of being simple and fast to run demanding very little computer time. The disadvantage is that this simple model is only able to reproduce the previously observed conditions/relationships contained in the historical data used to fit the model. In other words, the empirical model assumes the relationship between the predictor and predictand remain unchanged, an assumption that might not necessarily hold in the future. Despite this disadvantage, the empirical modelling approach here employed was considered novel enough to explore the feasibility of producing probabilistic rainy season onset forecasts for São Paulo.

In order to address the questions posed in the introduction the skill of the empirical Cox-regression model, the dynamical GloSea5 model and the combination of these two model forecasts was assessed and compared over a common period (1996–2009). Three approaches presented similar discrimination ability of around 80% for successfully distinguishing earlier from later than historical mean onsets in São Paulo, highlighting the potential and feasibility for producing skilful forecasts, despite the simplicity of the employed methods, particularly the procedure proposed for producing consolidated forecasts. The robustness of this assessment for an extended period (longer than 1996–2009) and for a region (20°S, 25°S, 45°W, 55°W) that includes the city of São Paulo was checked, reinforcing the validity of the obtained results at both local and regional scales. The assessment presented in this study was focused on probabilistic forecasts for the rainy season onset to be earlier or later than the historical mean onset, but the employed methods provide full PDFs or PEFs and therefore allow the production of forecast probabilities for any pre-defined timing threshold of interest.

Another relevant question is how comparable are the Cox-regression onset forecasts produced in this study to those produced with the traditional linear regression model. This question was addressed by fitting a simple linear regression model to the training period (1934–1995) and assessing the skill of the produced forecasts over the common validation period (1996–2009) to all models here investigated. The result indicated similar discrimination ability (81%) to the Cox-regression model (82%). This equivalence might not hold for other data sets, especially for situations when the predictand *versus* predictor relationships are non-linear and/or the time to onset distributions are non-symmetric. The main advantage of the Cox

regression over the linear regression is that the former is formulated in order to naturally model probability distributions rather than to produce a point estimate. Furthermore the Cox regression, as a semi-parametric model, does not require distributional assumptions for the response variable (time to onset) in contrast to the ordinary linear regression model that requires the normality assumption. Furthermore, for non-symmetric time to onset distributions, ordinary linear regression is not recommended because in such situations the normality assumption is violated.

The research performed in this study is aligned with one of the goal of the Global Framework for Climate Services (GFCS, Hewitt *et al.*, 2012) which is to enable better management of the risks of climate variability through the development and incorporation of science-based climate information and prediction into planning, policy and practice on the global, regional and national scale. The application of the science knowledge produced in this research has the potential to help National Meteorological and Hydrological Services (NMHSs) and World Meteorological Organization (WMO) Regional Climate Center (RCCs) to deliver improved tailored climate services at national and regional levels as good quality rainy season onset forecasts is a long standing demand by NMHSs and RCCs.

Acknowledgements

The research leading to these results has received funding from the Seasonal-to-decadal climate Prediction for the improvement of European Climate Services (SPECS) project (grant agreement no 308378) funded by the European Commission's Seventh Framework Research Programme. CASC was supported by Conselho Nacional de Desenvolvimento Científico e Tecnológico (CNPq) process 306863/2013-8. We also acknowledge the support provided by Fundação de Amparo à Pesquisa do Estado de São Paulo (FAPESP) Process 2015/50687-8 (CLIMAX project). The Institute of Astronomy, Geophysics and Atmospheric Sciences (IAG) of the University of São Paulo (USP) is acknowledged for making their precipitation data records available for the research performed in this study. We thank the comments, suggestions and constructive criticism of two anonymous reviewers that helped improve substantially the quality of this article.

References

Alves LM, Marengo JA, Júnior HC, Castro C. 2005. Início da estação chuvosa na região sudeste do Brasil: Parte 1 – estudos observacionais. *Rev. Bras. Meteorol.* **20**(3): 385–394.

Arribas A, Glover M, Maidens A, Peterson K, Gordon M, MacLachlan C, Graham R, Fereday D, Camp J, Scaife AA, Xavier P, McLean P, Colman A, Cusack S. 2011. The GloSea4 ensemble prediction system for seasonal forecasting. *Mon. Weather Rev.* **139**: 1891–1910, doi: 10.1175/2010MWR3615.1.

Bradburn MJ, Clark TG, Love SB, Altman DG. 2003a. Survival analysis part II: multivariate data analysis – an introduction to concepts and methods. *Br. J. Cancer* **89**: 431–436.

Bradburn MJ, Clark TG, Love SB, Altman DG. 2003b. Survival analysis part III: multivariate data analysis – choosing a model and assessing its adequacy and fit. *Br. J. Cancer* **89**: 605–611.

Camberlin P, Diop M. 2003. Application of daily rainfall principal component analysis to the assessment of the rainy season characteristics in Senegal. *Clim. Res.* **23**: 159–169.

Chen M, Shi W, Xie P, Silva VBS, Kousky VE, Higgins RW, Janowiak JE. 2008. Assessing objective techniques for gauge-based analyses of global daily precipitation. *J. Geophys. Res.* **113**: D04110, doi: 10.1029/2007JD009132.

Coelho CAS, Uvo CB, Ambrizzi T. 2002. Exploring the impacts of the tropical Pacific SST on the precipitation patterns over South America during ENSO periods. *Theor. Appl. Climatol.* **71**: 185–197.

Coelho CAS, Cardoso DHF, Firpo MAF. 2016. Precipitation diagnostics of an exceptionally dry event in São Paulo, Brazil. *Theor. Appl. Climatol.* **125**(3): 769–784.

Cox DR. 1972. Regression models and life-tables (with discussion). *J. R. Stat. Soc.* **34B**: 187–220.

Franchito SH, Rao VB, Barbieri PRB, Santo CME. 2008. Rainy-season duration estimated from OLR versus rain gauge data and the 2001 drought in Southeast Brazil. *J. Met. App. Clim.* **47**: 1493–1499.

Grambsch PM, Therneau TM. 1994. Proportional hazards tests and diagnostics based on weighted residuals. *Biometrika* **81**: 515–526.

Grimm AM, Ferraz SET, Gomes J. 1998. Precipitation anomalies in Southern Brazil associated with El Nino and La Nina events. *J. Clim.* **11**: 2863–2880.

Hewitt C, Mason SJ, Walland D. 2012. The global framework for climate services. *Nat. Clim. Change* **2**: 831–832.

Hosmer DW, Lemeshow S. 1999. *Applied Survival Analysis: Regression Modelling of Time to Event Data*. Wiley: New York, NY.

Jones C, Carvalho LMV, Liebmann B. 2012. Forecast skill of the South American monsoon system. *J. Clim.* **25**: 1883–1889, doi: 10.1175/JCLI-D-11-00586.1.

Liebmann B, Camargo SJ, Seth A, Marengo JA, Carvalho LMV, Allured D, Fu R, Vera CS. 2007. Onset and end of the rainy season in South America in observations and the ECHAM 4.5 atmospheric general circulation model. *J. Clim.* **20**: 2037–2050.

Lo F, Wheeler MC, Meinke H, Doland A. 2007. Probabilistic forecasts of the onset of the North Australian wet season. *Mon. Weather Rev.* **35**: 3506–3520, doi: 10.1175/MWR3473.1.

MacLachlan C, Arribas A, Peterson KA, Maidens A, Fereday D, Scaife AA, Gordon M, Vellinga M, Williams A, Comer RE, Camp J, Xavier P, Madec G. 2015. Global Seasonal forecast system version 5 (GloSea5): a high-resolution seasonal forecast system. *Q. J. R. Meteorol. Soc.* **141**: 1072–1084, doi: 10.1002/qj.2396.

Maia AH, Meinke H. 2010. Probabilistic methods for seasonal forecasting in a changing climate: Cox-type regression models. *Int. J. Climatol.* **30**: 2277–2288.

Mason I. 1982. A model for assessment of weather forecasts. *Aust. Meteorol. Mag.* **30**: 291–303.

Moron V, Robertson AW, Boer R. 2009. Spatial coherence and seasonal predictability of monsoon onset over Indonesia. *J. Clim.* **22**: 840–850, doi: 10.1175/2008JCLI2435.1.

Rayner NA, Parker DE, Horton EB, Folland CK, Alexander LV, Rowell DP, Kent EC, Kaplan A. 2003. Global analyses of sea surface temperature, sea ice, and night marine air temperature since the late nineteenth century. *J. Geophys. Res.* **108**(D14): 4407, doi: 10.1029/2002JD002670.

Ropelewski CF, Halpert MS. 1987. Global and regional scale precipitation patterns associated with the El Niño SouthernOscillation. *Mon. Weather Rev.* **115**: 1606–1626.

Ropelewski CF, Halpert MS. 1989. Precipitation patterns associated with the high index phase of the Southern Oscillation. *J. Clim.* **2**: 268–284.

Ropelewski CF, Halpert MS. 1996. Quantifying Southern Oscillation–precipitation relationships. *J. Clim.* **9**: 1043–1059.

Schoenfeld D. 1982. Partial residuals for the proportional hazards regression model. *Biometrika* **69**: 239–241, doi: 10.1093/biomet/69.1.239.

Vellinga M, Arribas A, Graham R. 2013. Seasonal forecasts for regional onset of the West African monsoon. *Clim. Dyn.* **40**: 3047–3070, doi: 10.1007/s00382-012-1520-z.